R & D for High Energy Gamma-Ray Telescope using Scintillation Fiber with Image Intensifiers

T.Sako ^{a,1}, Y.Muraki ^a, Y.Matsubara ^a, M.Sato ^a, K.Niwa ^b, M.Nakamura ^b, S.Sato ^b, T.Nakano ^b, Y.Tanaka ^b and H.Okuno ^c

^b Dep. of Physics, Nagoya University, Nagoya 464-01, Japan

¹ e-mail:sako@stelab.nagoya-u.ac.jp.

A new gamma-ray telescope using scintillation fiber together with an image intensifier is presented. The image intensifier we used has been improved in the sensitive range of the wavelength (beyond 300nm) and the quantum efficiency (maximum 20%). The results of the beam test using the accelerator and the Monte Carlo simulation for the prototype telescope show that the device has the angular resolution of 0.5 degree at 900MeV. On the basis of results of the prototype telescope, we propose a new SCIFI (SCIntillation FIber) telescope for future gamma-ray astronomy. The new telescope has achieved a large solid angle. With this merit, the new telescope can investigate very dark gamma-ray sources and monitor transient events such as gamma-ray burst. In addition, the cost of devices used in the telescope is not expensive so that an extension of the area of the telescope is easily realized in comparison with telescopes using silicon detector such as GLAST.

^a Solar-Terrestrial Environment Laboratory, Nagoya University, Furo-cho, Tikusa-ku, Nagoya 464-01, Japan

^c Institute for Nuclear Study, University of Tokyo, Tokyo 188, Japan

1 Introduction

One of great mysteries of astrophysics is 'where and how are cosmic rays accelerated?'. This notable problem has not yet been resolved since their discovery by Hess [1]. However at that time it was not known that our universe is filled by magnetic fields. Today, having learned of the existence of magnetic field in space, we know that if we wish to find the sources of cosmic ray acceleration, we should exploit neutral particles such as gamma-rays, neutrons and neutrinos.

From this point of view, there has been considerable progress with the use of Cherenkov techniques [2, 3] in observing gamma-rays around the TeV region. In fact the existence of gamma-rays emitted from Crab nebula and even from the extragalactic source Mk421 has been established [4]. These results strongly indicate that the acceleration of electrons to very high energies frequently involves the inverse Compton process. The accelerated electrons collide with background photons and these can be detected by Cherenkov telescopes at the ground. However there remain many uncertainties connecting the origin and acceleration of protons and heavy primaries.

Previously it was believed that Cyg X-3, associated with a Wolf-Rayet star, could be a major source of cosmic rays [5, 6, 7]. In fact an increased intensity of cosmic rays observed from this object coincided with a large radio flare in January 1991 [8, 9]. The increase was thought to have been possibly caused by the arrival of very high energy neutrons.

However the observations of Cygnus X-3 made by CGRO and the COS-B satellite in the GeV region are confusing [10, 11]. They certainly observe an increase of flux around the Cygnus region and have even found three bright point sources there. In case of the CGRO EGRET experiment, of 9 bright spots with more than 6 sigma statistical significance, three are in Cygnus region. However if we consider the background to be expected from collisions between cosmic-rays and a molecular cloud, it is unclear whether high energy cosmic rays are really coming from Cygnus X-3.

We require further observations of this object using a detector with good angular resolution and a large sensitive area. The detector system must be stable and also economical. For such a purpose we have previously proposed using a silicon calorimeter [12, 13] which has been used in the CERN UA7 experiment [14]. However in this paper we wish to report another endeavor to use scintillation fiber

together with an image intensifier as a read-out system. In section 2, we describe briefly our prototype gamma-ray telescope fabricated with the use of scintillation fiber and in Section 3 and 4, we describe the results obtained using photon beams at the Institute for Nuclear Study of the University of Tokyo. In Sections 5,6 and 7, we present a design for large-scale gamma-ray detector using scintillation fiber and the image intensifier. A summary and conclusions are given in section 8. The accelerator experiments were carried out in April and June of 1993 at Institute for Nuclear Study of the University of Tokyo.

2 Prototype Telescope

The gamma-ray telescope must have two main functions: determination of the arrival direction of gamma rays and measurement of each photon energy. The incoming photons are converted into electron pairs inside the target. However if a thick converter is used as a target, the electron pairs are largely deflected inside the target material by multiple Coulomb scattering and the pointing accuracy of the gamma-ray telescope will be largely lost.

In order to resolve this problem, it would be ideal in the design of the gamma-ray telescope to use a target such as a scintillation fiber. However the radiation length of the scintillation fiber is more than 40 cm, so the conversion rate of photons into electron pairs is depressed by the use of this material. In the test experiment, we have used a sandwich type target with a sheet of scintillation fiber of 500 μ m thickness and a lead plate of 5mm thickness as shown in Fig.1. The telescope has been tested in photon beams of Institute for Nuclear Study of the University of Tokyo during May 1993. This paper describes the results obtained by the test experiment.

Electron pairs converted in the scintillation fiber (or lead plate) travel 20 cm and arrive at the calorimeter as shown in Fig.1. The photon energy is measured by means of the calorimeter. The calorimeter consists of a lead plate with thickness 5mm and the sheets of the scintillation fiber which are arranged in the perpendicular direction. The high energy electron and positron produce a pair of electron showers inside the calorimeter and their energies are measured by the traditional cascade technique. The center of the two showers is determined using the information obtained from the scintillation fibers. The signal is converted into total pulse height by an integration of each photon with use of the information coming from an image

intensifier attached to the bundle of scintillation fiber.

The incoming direction of gamma-rays is obtained by constructing a straight line between the conversion point of the incident gamma-ray photon into an electron pair and the center of gravity of the two photon showers. Charged particles can be rejected by the use of the signal coming from the scintillation counter located on the top side of the telescope.

We describe in more detail the characteristics of the scintillation fiber and the image intensifier used. The scintillation fiber used in the prototype telescope is KURARAY SCSF38 with fiber diameter 500 μ m. This is composed of a polystyrene core (refractive index n=1.59) with 470 μ m radius clad with poly-methylmeta-acrylate (n=1.49) of thickness 15 μ m. The attenuation length of photons inside the fiber is estimated as 200 cm. Sheets of scintillation fiber were made by binding fibers around a drum (85 cm diameter) and cutting them into flat pieces. The surface of the drum is grooved at intervals of 500 μ m [15]. The fibers were fixed by painting them with a white aclyric-emulsion paint. The size of the scintillation fiber sheet is 88 mm in width, 850 mm in length with 3 mm in thickness (7 layers of fibers). Twelve sheets were produced. One edge of the scintillation fiber sheet is connected to the image intensifier. The edge was polished by a diamond cutter.

The image intensifier (abbreviated as I-I) is used as a device for measuring the photons emitted from scintillation fibers. The I-I (V4440P-UVFX) has been made at HAMAMATSU in a collaboration with the group of the Physics Department of Nagoya University. In a normal image intensifier, a material is doped in the front glass to absorb photons with large angle of inclination which make the position resolution worth. In this experiment we do not need such precise positional resolution as 20 μ m, which is smaller than the diameter of a fiber. By avoiding the use of doping material in the front glass, two characteristics have been improved: the observation range has been greatly stretched into the UV region and goes beyond 300 nm and the quantum efficiency has also been improved. As shown in Fig.2, the efficiency is nearly doubled in comparison with the previous tube (V4440P) to a value comparable to that of photomultipliers. The diameter of a window of the present I-I is 10 cm so that a large size image can be recorded with a single I-I.

The present I-I consists of three cascades of I-Is. In the first stage of the I-I, the image is reduced to 2.5 cm diameter using an electron lens. The following two I-Is intensify the image with a maximum gain of 3×10^3 in each I-I. A CCD camera (C3077;HAMAMATSU) was used for the read-out of this 2.5 cm diameter image.

This camera has 768 pixels(in the horizontal direction) \times 493 pixels(in the vertical direction) and 50 pixels of the horizontal line are optically black. The size of a pixel is $11.0\mu m \times 13.0\mu m$. Through the optical lenses, almost all of the area of an image can be scanned.

3 Experimental Details

The scintillation fiber telescope was placed in the electron beam of the Institute for Nuclear Study of the University of Tokyo. Electrons accelerated hit a platinum target (thickness of 50 μ m) and produce gamma-rays as bremsstrahlung. The photon energy is measured by tagging the reflected electrons with use of a bending magnet as shown in Fig.3. The energy resolution of the photons is determined by measuring the positions of the tagged electrons. In the present experiment, this turns out to be \pm 5 MeV. The experimental arrangement and the trigger logic are shown schematically in Fig.4.

The photon beams are injected vertically at the center of the telescope. The telescope was also tested by the electron beam. A schematic diagram of the trigger logic is shown in Fig.4. In this case, electrons are also injected vertically at the center of the telescope. The energies of photon beam and electron beam are summarized in Table.1, together with the number of events triggered.

Photon beams are used to investigate the pointing accuracy of the telescope and the energy resolution is investigated with use of electron beams. More details of the INS electron accelerator are to be found in Reference [16].

4 Experimental Results

One of the events observed with use of present system is shown in Fig.5a. Four groups of bright spots can be recognized at the center of the screen. These correspond to points where pair conversion occurred and the region where showers developed in the calorimeter: both are seen from X-direction and Y-direction. The isolated dots surrounding these lumps of photons are associated with CCD noise. The X-direction and Y-direction scintillation fibers are combined and are observed by a single image intensifier.

In Fig.5b, a simulated CCD image is presented. In constructing this diagram, photons from showers and also CCD noise are included. The simulated event shown

in Fig.5b reproduces the observed results quite well (Fig.5a).

We now explain how the photon energy and direction of incident can be extracted with use of actual data. A clump of pixels connected with each other was considered to form one cluster. Any cluster which contains less than 70 pixels was regarded as noise and was rejected. In reality, the image obtained by the image intensifier is usually distorted and a correction procedure must be considered. We have used a test pattern to correct for this distortion: from a test pattern really seen by the I-I we have obtained the spatial correction coefficient for each position. After correcting the spatial distribution by this means, the image was divided into 12 parts corresponding to the 12 sheets of scintillation fiber.

The open squares of Fig.6 represent experimental results on the angular resolution of the present scintillation fiber telescope. The result is obtained by combining the conversion point of photons into electron pairs and the center of gravity of two photon showers by a straight line. Each direction derived shows Gaussian distribution with a unit of photons per degree per stradian. The origin of this distribution is defined by the mean direction of all events, and the angular resolution is defined by HWHM of this distribution. The result of the simulation obtained using the EGS4 program has been also shown in Fig.6 by the filled squares. From Fig.6, the angular resolution is seen to be less than 0.7 degree at E=900 MeV. In simulating photon showers with use of the EGS4 program, the following points are taken into account:

- 1) One photon yield is assumed to every 200 eV energy deposited in the scintillation fiber.
- 2) Because the critical angle of reflection in the fiber is 20 degree, the probability that a scintillation photon can face the surface of the I-I is assumed to be,

$$\frac{2\pi(1-\cos 20)}{4\pi} = 0.03$$

3) Because the attenuation length of photons in the fiber is 200 cm, the survival probability of photons after passage of 80 cm (a typical length from the interaction region to the I-I surface) in the fiber is

$$exp(\frac{-80}{200}) = 0.67$$

4) The quantum efficiency of the window of the I-I is 20

- 5) The accuracy of position determination is reduced to 500 μ m which is the fiber diameter.
- 6) One photoelectron is amplified by the I-I and a spot is made with FWHM of 1 mm
- 7) An average of thirty random spots are assumed as noise in a screen for one event.

As a result of this procedure, the screen image of the simulation clearly approaches the experimental data. These simulated images were also analyzed with software used in analyzing real images obtained by the experiment. The angular resolution deduced by the simulation is also shown in Fig.6. Though there is a difference of factor around 0.9 between the experimental result and the simulation, the results of the latter are consistent with experimental results. The minor difference is considered to arise from contamination of the image as a consequence of the high beam density used in the experiment.

The experimental results of Fig.6 (open squares) suggest that the angular resolution of the telescope saturates at the highest energy (E=900MeV). The expected angular resolution based on the Monte Carlo calculation is marked (filled squares) in Fig.6. This limit on the angular resolution arises from the fluctuation of the photon beam itself. At the entrance of the telescope, the conversion points are scattered within a circle of 10 mm radius. Because the distance between the point from where the beam emerged and the telescope was 1510 mm, the beam can fluctuate about 0.4 degree(10/1510 radian). In fact, when a Monte Carlo calculation is made without taking account of this beam spread, the angular resolution turns out to be 0.5 degree at 900 MeV. This result is shown in Fig.6 by a small filled square.

Cascade theory indicates that the total track length determined by a calorimeter is proportional to the incident electron and photon energy. In the present experiment, this principle is also applied using the sum of the respective ADC values measured by each scintillation fiber. If we denote the mean number of photons induced by the shower with an energy E by N(E), then the energy resolution of the calorimeter is defined by $\sqrt{N}/N(E)$. In this case, N(E) is proportional to E so that the energy resolution can be represented as a/\sqrt{E} . The data obtained on the energy resolution is given in Fig.7 as a function of the primary electron energy E.

The data are fitted to a function of the form $\Delta E(\%) = a/\sqrt{E(GeV)} + b$, as shown by the curve in Fig.7; the parameters which describe the energy resolution of the calorimeter are found to be a=13.7 % and b=15.0 %. The large constant

term (b=15 %) is a consequence of the limited thickness of the scintillation fiber and the poor linearity of the gain of the I-I. If we use a thicker calorimeter or a position sensitive photomultiplier as a read-out device, the energy resolution will be much improved.

5 A Proposal for Gamma-ray Telescope using Scintillation Fibers

Within a few years, the EGRET detector carried on CGRO satellite will be obsolete and a new kind of gamma-ray detector will become necessary. Such a new generation gamma-ray telescope is proposed here based on a Monte Carlo simulation and existing experimental data. The software used in the present Monte Carlo simulation has been confirmed by our accelerator experiment, so the expected results should be very reliable.

The proposed new gamma-ray telescope consists of scintillation fibers with image intensifiers as the read-out system. A schematic view of the proposed telescope is shown in Fig.8a and b. One of the main differences in comparison with the CGRO EGRET detector is the large area of the acceptance. In the form of the EGRET detector and also the COS-B and SAS-2 satellites, a scintillator dome is used to reject the enormous flux of charged cosmic-rays by anti-coincidence. In the present design, the top surface of the scintillation fiber (or a plastic scintillator) is used for discriminating gamma-rays from cosmic-rays and the signals from the top array of the fiber are sensed by the photomutiplier as shown in Fig.8a and 9. The trigger pulse given to the image intensifier is created by the pulse from the scintillation fiber with use of the logic shown in Fig.9. By this method, a large solid angle is guaranteed.

Ten layers of lead plate converter with thickness 250 μ m are used for the Monte Carlo calculation. This permits good angular and energy resolution. In the Monte Carlo study, we have set as a first priority, good angular resolution of the telescope and enough event rates to provide good statistics.

The decay time of a image of present image intensifier is about 20 μ sec in which time cosmic rays leave many tracks in an image. We can technically reduce the decay time to about 100 nsec in which time the expected number of cosmic rays is about one event. With use of software, tracks left by cosmic rays can be rejected. Both the 20 μ sec and 100 nsec imply that the dead time of the proposed device is essentially zero, whereas that of EGRET is 110 msec.

6 Results of Monte Carlo Calculations of the New Telescope

The angular resolution and the detection efficiency of the new telescope are shown in Fig.10 and 11 respectively. The incoming direction of photons is determined by constructing a straight line between the conversion point and shower center. The trigger logic is shown in Fig.9. The detection efficiency is divided into two stages. The first stage, named 'trigger efficiency', is defined as the ratio of the number of triggered events to the number of incident gamma rays. The second, named 'imaging efficiency' is defined as the ratio of the number of selected events in the image analysis to the number of incident gamma rays. The image analysis was carried out completely with the software described in part in section 3. The energy resolution, defined as the root mean square, is shown in Fig.12. Using NaI with 10 radiation lengths, the energy resolution of the telescope can be improved to better than 10 % at 20 GeV.

The main features of present telescope proposed are summarized as follows: (1) The angular resolution is about 1 degree at 1GeV, (2) the energy resolution is expected to be 6% at 1 GeV, (3) a uniform detection efficiency of 25% is realized over a wide energy band, (4) a large acceptance of the telescope $(1.5m^2 \text{ sr})$ is possible, and (5) perhaps most importantly the level of technology and the cost of construction are quite acceptable.

7 Advantages of the SCIFI Telescope

The properties of the new SCIFI (SCIntillation Fiber) telescope are summarized in Table.2 for comparison with the properties of EGRET detector and GLAST proposal [17, 18]. The most advanced property of the present telescope is to be found in the large solid angle achieved. The expected statistics for point source searches in the case of all sky survey with use of present telescope is shown in Table.3. The duration of an all sky survey is assumed to be 19 months as in the case of the EGRET observations. Table.3 indicates that a very dark gamma-ray source which the EGRET detector could not see, can be resolved with present telescope.

Here we note an important point. Because the scintillation fiber is composed of polystyrene, solar neutrons can be detected. Neutrons entering the telescope knock out hydrogen nuclei (protons) from the polystyrene and such events can pass the

previous trigger logic (Fig.9).

In comparison with GLAST, the SCIFI telescope has somewhat inferior angular resolution, however the acceptance and the energy resolution is the same order. The acceptance is about 25 times larger than that of the EGRET detector. The volume is twice that of GLAST, because of large volume of I-Is, however the total weight of the telescope is only two thirds that of GLAST.

One of the most important advantages can be seen in the cost, which is only about 4 % of that of GLAST.

8 Summary

We have developed high energy gamma ray telescopes using scintillation fibers and image intensifiers. Firstly, we have designed and constructed a prototype telescope with use of these materials. From the results of beam tests, we conclude that the device is useful for future gamma-ray telescopes. Other investigations have previously made of a high energy gamma ray telescope using scintillation fiber [19], but the present experiment is the first to use a gamma ray beam.

Simulations of the properties of the scintillation fiber combined with the image intensifier have been made using the EGS4 Monte Carlo code.

On the basis of results of experiments we have proposed a new SCIFI telescope. Because of the use of scintillation fiber in the converter as the trigger, a very large solid angle of the telescope can be realized. With this telescope, very dark gamma ray sources, as shown in Table.3, can be investigated. Furthermore, by monitoring a wide field of view it is possible to study many transient events such as gamma ray bursts and active galactic nuclei.

Since scintillation fiber is not expensive, the present type of telescope can be more easily enlarged in comparison with telescopes using silicon detectors such as GLAST. In planning the construction of a large area telescope (over $10m^2$), the SCIFI telescope offer the most realistic approach.

Acknowledgements

We acknowledge the assistance of the staff of the Electron Synchrotron(ES) at the Institute for Nuclear Study, the University of Tokyo. In particular K. Watanabe guided us in the operation of the machine. Professor P.V.Ramana Murthy provided us many useful suggestions on the practical design of the telescope.

The authors thanks to Professor Ian Axford for careful reading of the manuscript. The Monte Carlo simulation was done using the FACOM M780 at the Computer Room, the Institute for Nuclear Study, the University of Tokyo.

References

- [1] V.F.Hess, Physik Zentschr. 13(1912)1084.
- [2] G.Vacanti et al., Astrophys. J. 377(1991)467-479.
- [3] T.Kifune et al., Astrophys. J. 438(1995) L92-L94.
- [4] M.Punch et al., Nature (1992) 477-478.
- [5] M.Samorski and W.Stamm, Astrophys. J. 268 (1983) L17-L21.
- [6] J.Wdowczyk and A.W.Wolfendale, Nature, 305(1983)609-610.
- [7] A.M.Hillas, Nature, 312(1984)50-51.
- [8] G.L.Cassiday et al., Phys.Rev.Lett.62(1989)383-386.
- [9] M.Teshima et al., Phys. Rev. Lett. 64(1990) 1628-1631.
- [10] W.Hermsen et al., Proc. 19th Internat. Cosmic Ray Conf. (La Jolla), 1,95(1985)
- [11] C.E.Fichtel et al., Astrophys. J. Suppl. 94(1994)551-581.
- [12] A.Nakamoto et al., Nucl. Instr. and Meth., A251(1986)275-285.
- [13] T.Kashiwagi et al., Nucl. Instr. and Meth., A290(1990)579-588.
- [14] J.Bourotte et al., Nucl. Instr. and Meth., A274(1989)129-133.
- [15] T.Nakano et al.,IEEE Trans.Nucl.Sci.,39(1992)680.
- [16] Inst. for Nuclear Study, the Univ. of Tokyo, 1.3 GeV Electron Synchrotron User's Guide (1993)
- [17] D.J. Thompson et al., Astrophys. J. Suppl. 86(1993)629.

- [18] P.F. Michelson, Towards a major atmospheric Cherenkov detector III.(1994)321.
- [19]S.Torii et al.,220/SPIE,1734(1992) Gamma-Ray Detectors.

Table Captions

Table.1 a)Beam intensity used for testing the angular resolution (counts per every 10 seconds.) and the number of events recorded. Tag sigma means the total number of electron passed by all tag counters and tag means the number of electrons passed one of the tag counters selected, corresponding to a fixed energy of gamma rays. b)Beam intensity used in testing the energy resolution (counts per every 10 seconds) and the number of events recorded.

Table.2 Properties of new SCIFI telescope in comparison with those of other telescopes. The budget of SCIFI telescope indicates the total cost of I-Is.

Table.3 The sensitivity for point source research in a 19 months all sky survey with the present telescope (S to \sqrt{N} ratio). The fluxes of diffuse gamma rays assumed to be $6.1 \times 10^{-4} photonscm^{-2}sec^{-1}sr^{-1}(> 100MeV)$ for the Galactic Center, 25% of the G.C. for the anti G.C., and 10% of the G.C. for high latitude

Figure Caption

Fig.1 The prototype SCIFI (SCIntillating FIber) telescope. Incident gamma rays are converted into an electron and positron pair in the lead converter. The position of the electron and positron pair is recorded with SCIFI sheets arranged perpendicularly. SCIFI sheets are also arranged in the part of the calorimeter. The directions of gamma rays are determined from the conversion point and the center of the gravity of the energy deposition.

Fig.2 The quantum efficiency of the image intensifier. The image intensifier V4440P-UVFX has high quantum efficiency over a wide range of wavelength. This can be improved by a change of the fiber optic plate.

Fig.3 The tag counter. Tagged electron indicates the energy of photon radiated.

Fig.4 The arrangement of the device used for beam tests. a) For the test of the angular resolution. b) For the test of the energy resolution. When a trigger signal was generated, a CCD image was recorded on a magnetic optical disk through an A/D converter.

Fig.5 An example of CCD images obtained in the case of the investigation of the angular resolution. a)The raw image. b)The simulated image. c)The procedure for image analysis. The image is divided into corresponding SCIFI sheets and the variations of the intensity along each sheet are derived. The first and second brightest peaks and the centers of gravity of each sheet are found. From the right side of the figure, the first two layers show the x coordinate of the SCIFI sheets in the converter part, the third and fourth layers show the y coordinate. The fifth and

sixth and the ninth and tenth indicate the x and the y coordinate at the entrance of the calorimeter, respectably. The seventh and eighth layers show the x coordinate in the calorimeter (after 2 and 4 radiation length, respectably) and the eleventh and twelfth layers show the y coordinate.

Fig.6 The angular resolution of the prototype telescope. The angular resolution is defined by HWHM of the distribution to the mean incident direction. Open squares show the experimental results. Filled squares show simulated results. The small filled square is a simulated result for a beam without angular fluctuation.

Fig.7 The energy resolution of present sampling calorimeter. The energy resolution is defined by root mean square of the sum of the ADC value. Filled circles show the experimental result. These data are fitted to the curve : $y = a/\sqrt{E(GeV)} + b$ with a=13.7 % and b=15.0 %.

Fig.8 The new SCIFI telescope. a) A schematic view of the new telescope which is composed of a conversion and a calorimeter. One of the edges of the SCIFI sheets is connected with the surface of the I-I for photon counting. Another edge of the sheets is connected with PMTs for generating trigger pulses. b) A part of new telescope. Photons are converted by ten layers of thin lead plates and SCIFI sheets arranged perpendicularly. Inorganic scintillator is used for the calorimeter and SCIFI sheets are arranged to derive the center of the gravity of showers.

Fig.9 Schematic diagram of the trigger logic. The trigger signal for recording the CCD image is generated using the luminescene of SCIFI in the converter. In present system TOF is not required and the field of view is enlarged.

Fig.10 The expected angular resolution defined by HWHM.

Fig.11 The detection efficiency of new telescope. Filled circles show the 'trigger efficiency'. Filled squares show the 'imaging efficiency'.

Fig.12 The energy resolution for a NaI scintillator having a thickness of 10 radiation lengths.

Electron energy (MeV)	Gamma-ray energy (MeV)	${\rm tag}\ \Sigma$	$_{ m tag}$	Number of events
400	100	77171	155	2221
400	250			1291
1000	600			1624
1000	900	43401	162	1781

Table 1

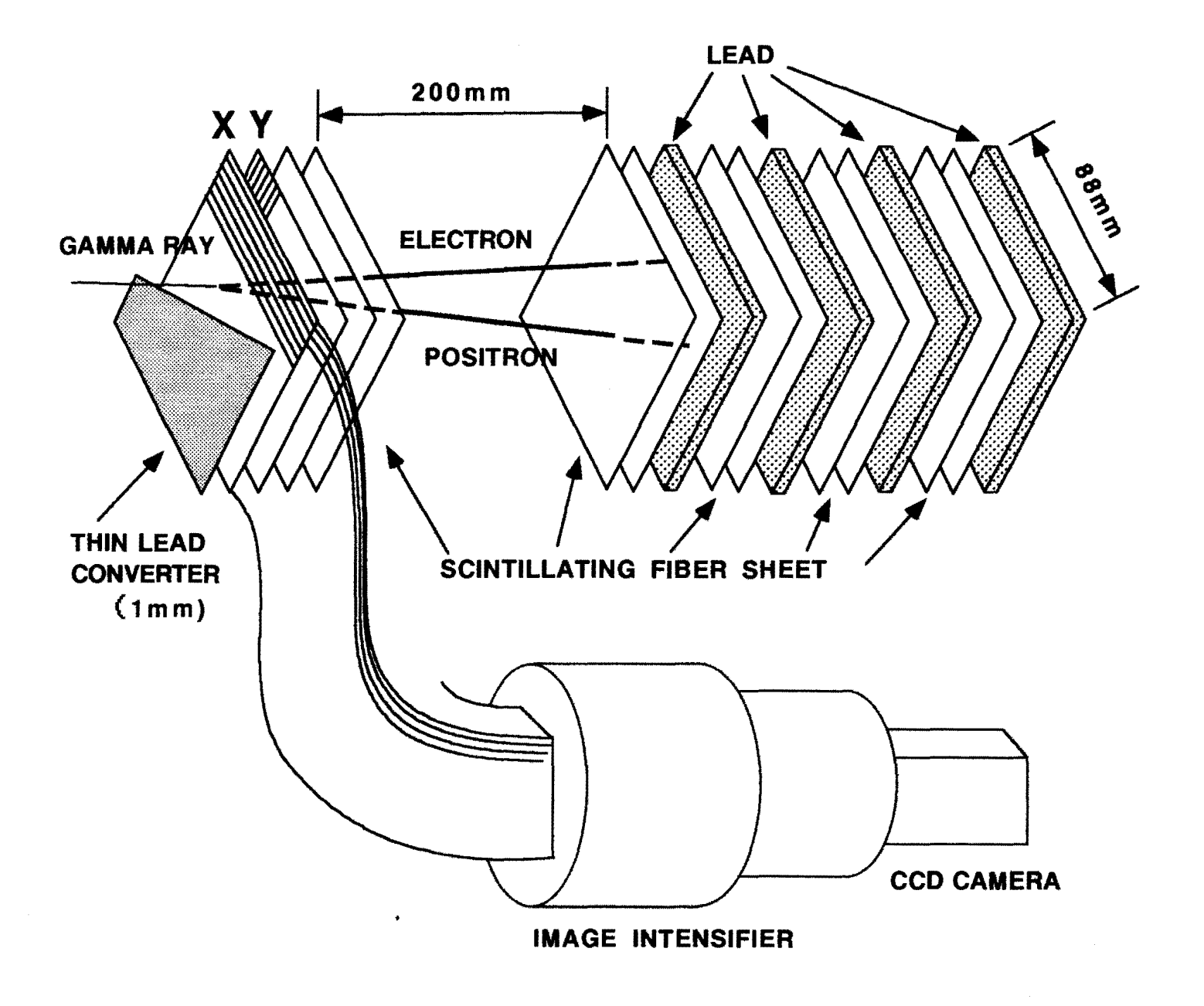
$\begin{array}{c} {\rm Electron\ energy} \\ {\rm (MeV)} \end{array}$	Intensity of electron beam	Number of events
150	13977、852	485
450	1609、360、21872、27892	485
700	1119	541

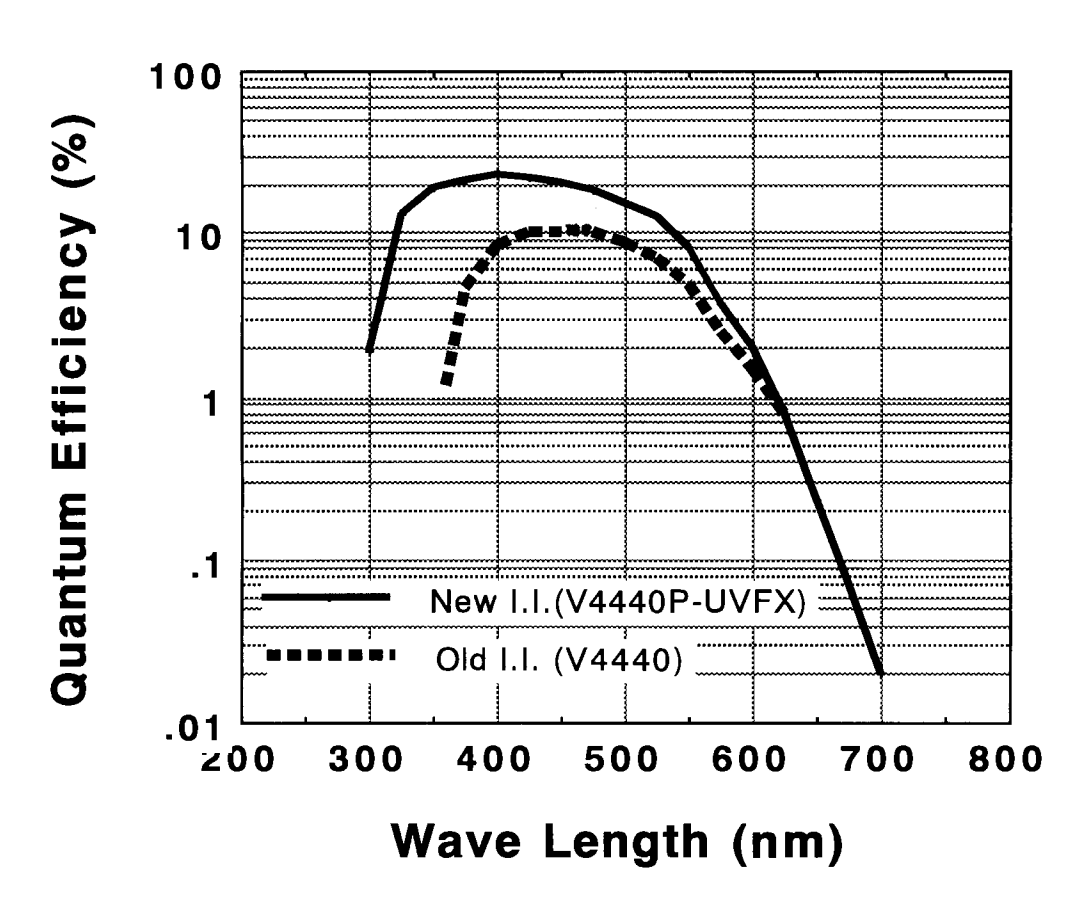
Position of	Intensity of	gamma-ray ($(10^{-7}cm^{-2}s^{-1})$	$^{-1}, > 100 MeV)$
gamma-ray source	3.0	1.0	0.5	0.3
Galactic center	11.1	3.7	1.9	1.1
Anti G.C.	22.3	7.4	3.7	2.3
High Galactic latitude	35.3	11.7	5.9	3.5

Table 3

Table 2

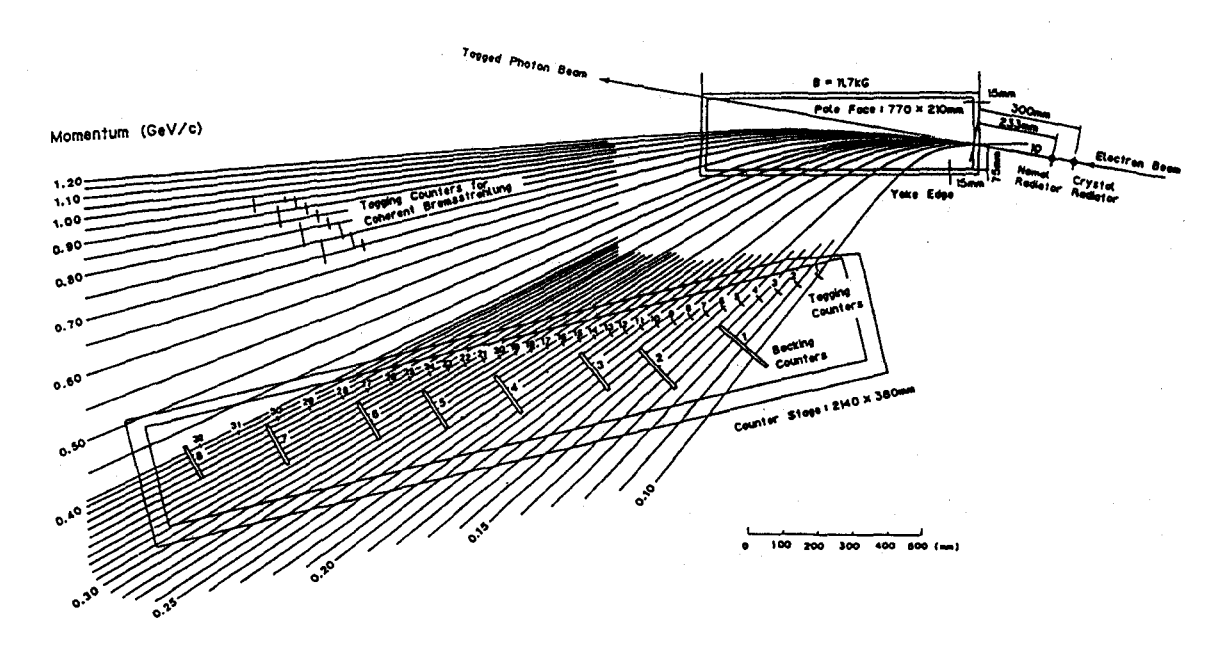
	EGRET	GLAST	SCIFI Telescope
Angular			
Resolution			
(degree)			
$0.1~{ m GeV}$	2.8	1.8	3.6
1.0 GeV	0.6	0.3	1.1
10.0 GeV	0.2	0.08	0.4
Energy			
Resolution		,	
0.1 GeV	13 %	8 %	16 %
1.0 GeV	9 %	4.4 %	5.5 %
10.0 GeV	12 %	6 %	8.9 %
Area	$0.65~\mathrm{m}^2$	$3.2~\mathrm{m^2}$	1.0 m^2
Effective	$0.025 \text{ m}^2 \text{ at } 50 \text{MeV}$	$0.50 \text{ m}^2 \text{ at } 50 \text{MeV}$	0.26 m ² at 0.1 GeV
Area	$0.12 \text{ m}^2 \text{ at } 1 \text{GeV}$	$0.88 \text{ m}^2 \text{ at } 1\text{GeV}$	$0.30 \text{ m}^2 \text{ at } 1 \text{GeV}$
Alea	$0.07~\mathrm{m^2}$ at $10\mathrm{GeV}$	$0.77 \text{ m}^2 \text{ at } 10 \text{GeV}$	$0.25~\mathrm{m^2}$ at $10\mathrm{GeV}$
Solid Angle	$0.08 \times 2\pi$ sr	$0.41 \times 2\pi \text{ sr}$	$0.77 imes 2\pi ext{ sr}$
Sensitivity	$0.06~\mathrm{m^2~sr}$	$2.3~\mathrm{m^2~sr}$	$1.5~\mathrm{m^2~sr}$
Volume	4.8 m^3	2 m^3	$4 \mathrm{m}^3$
Mass	1830 kg	3000 kg	2000 kg
Budget		\$ 100M	\$ 4M

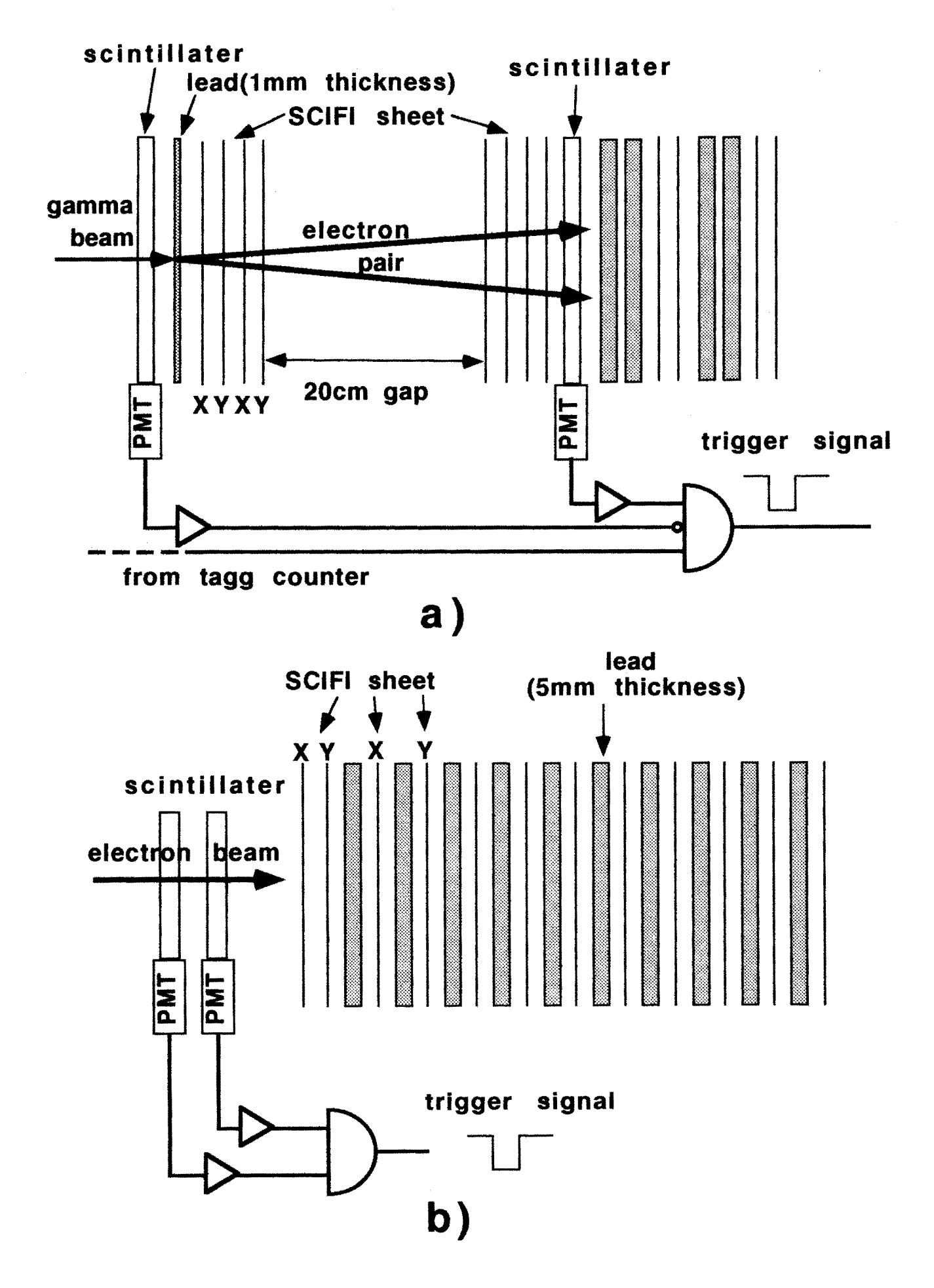




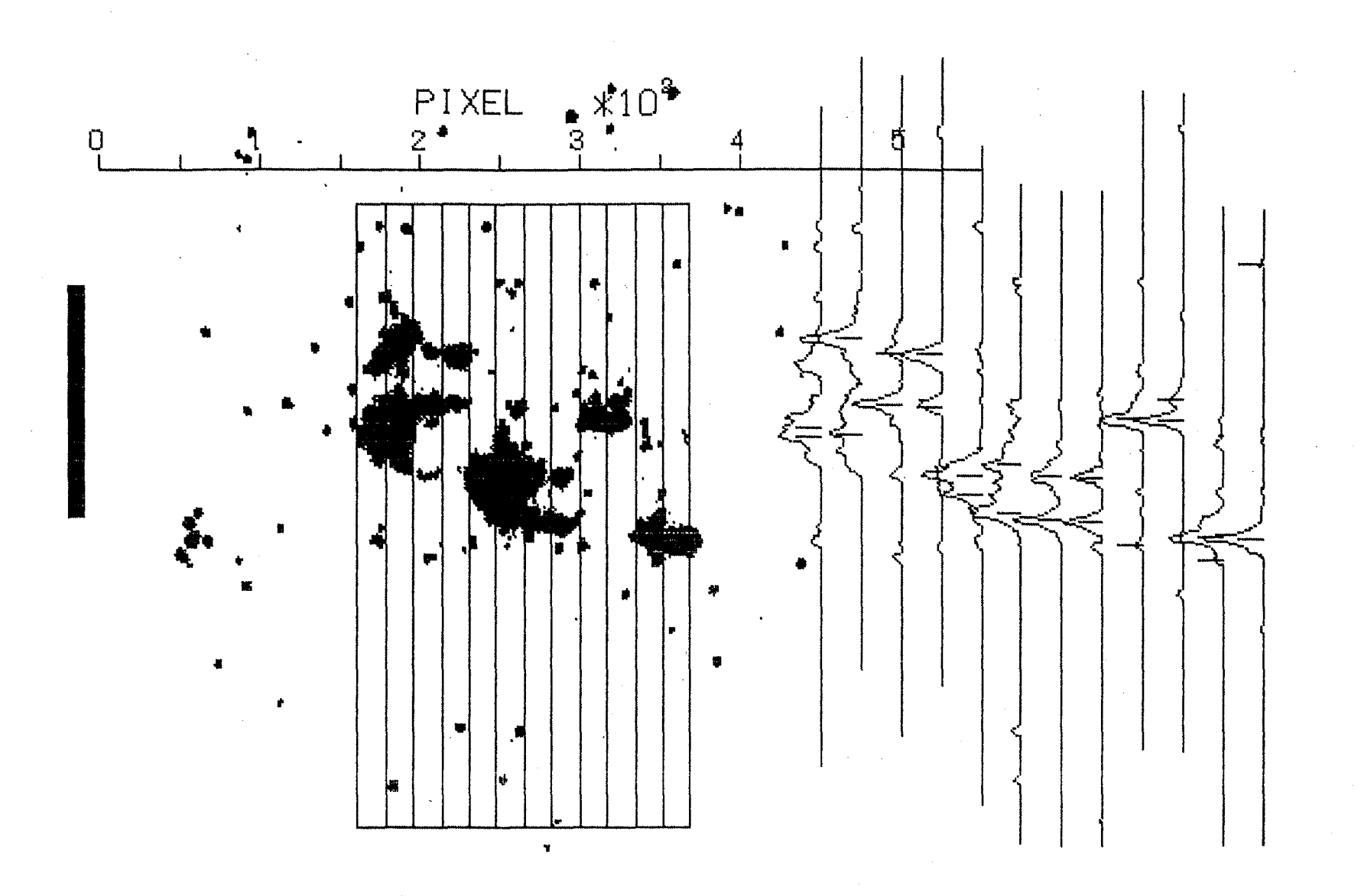


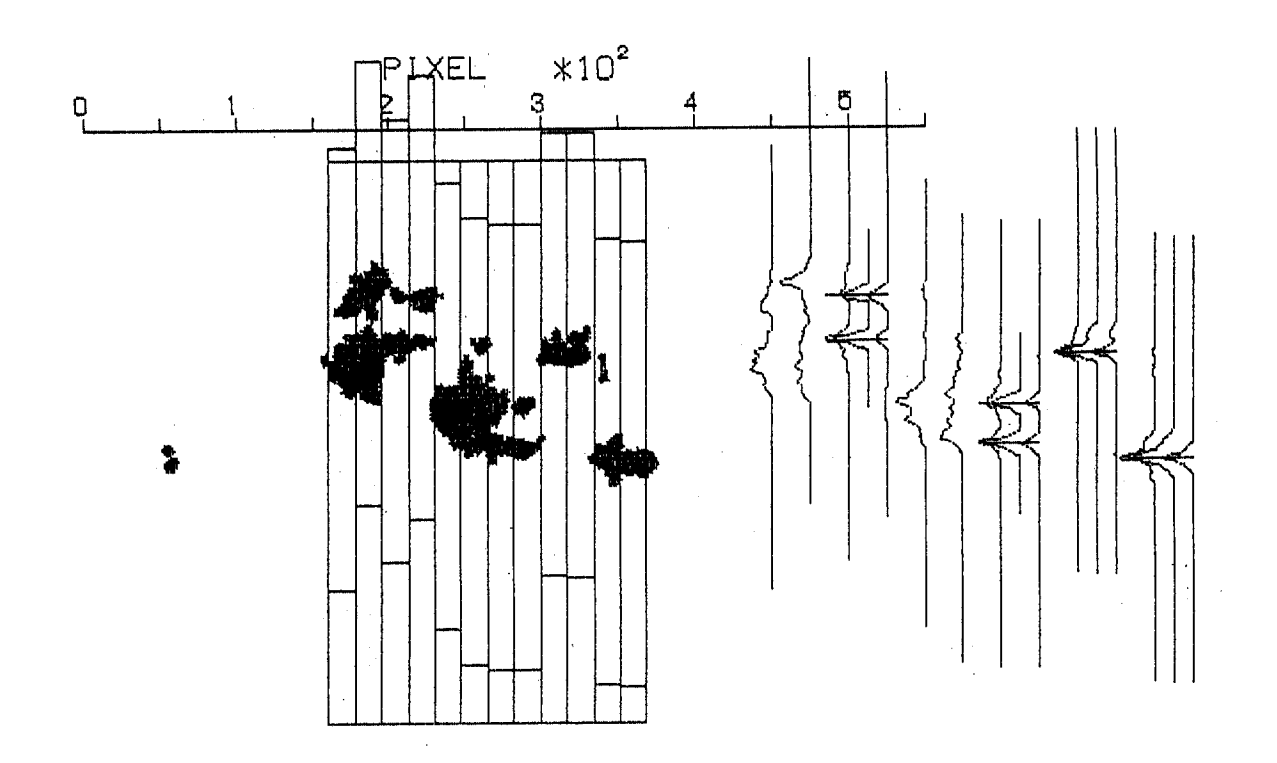
INS Photon Tagging System



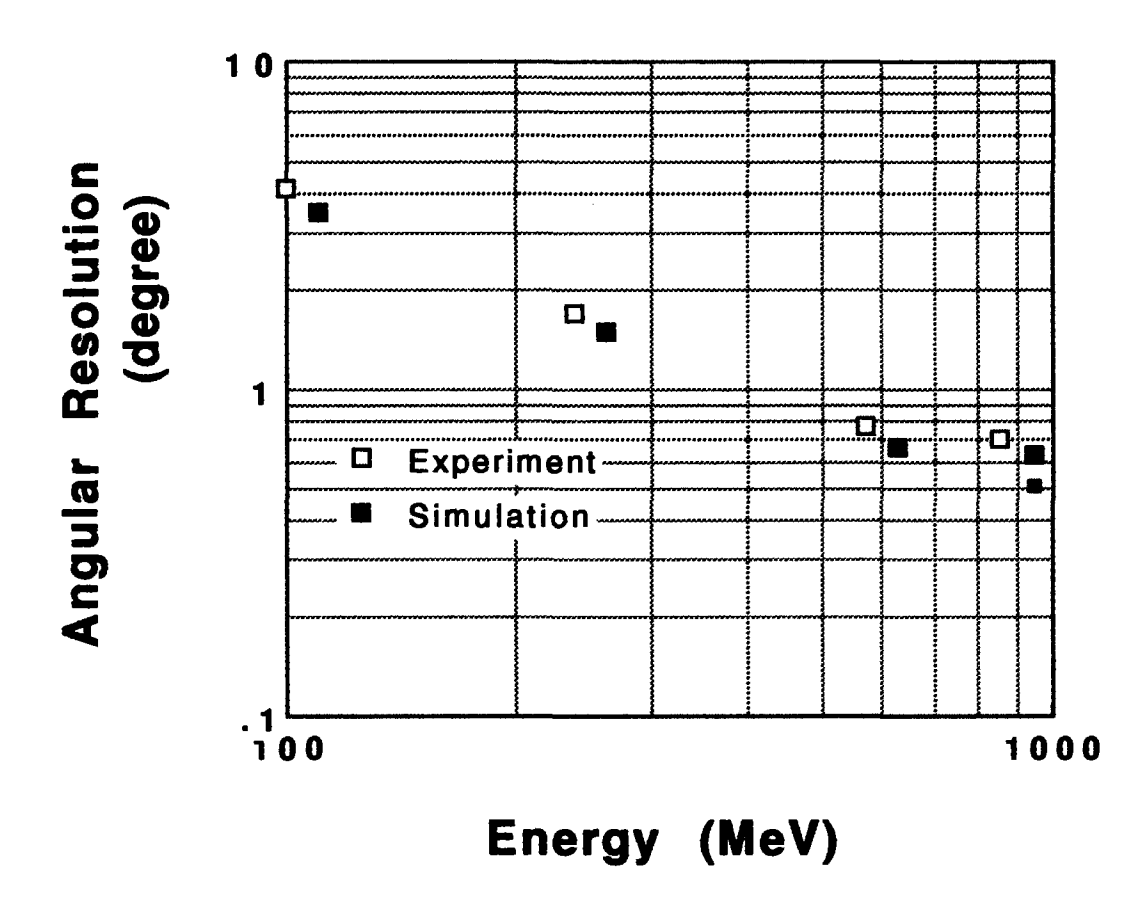




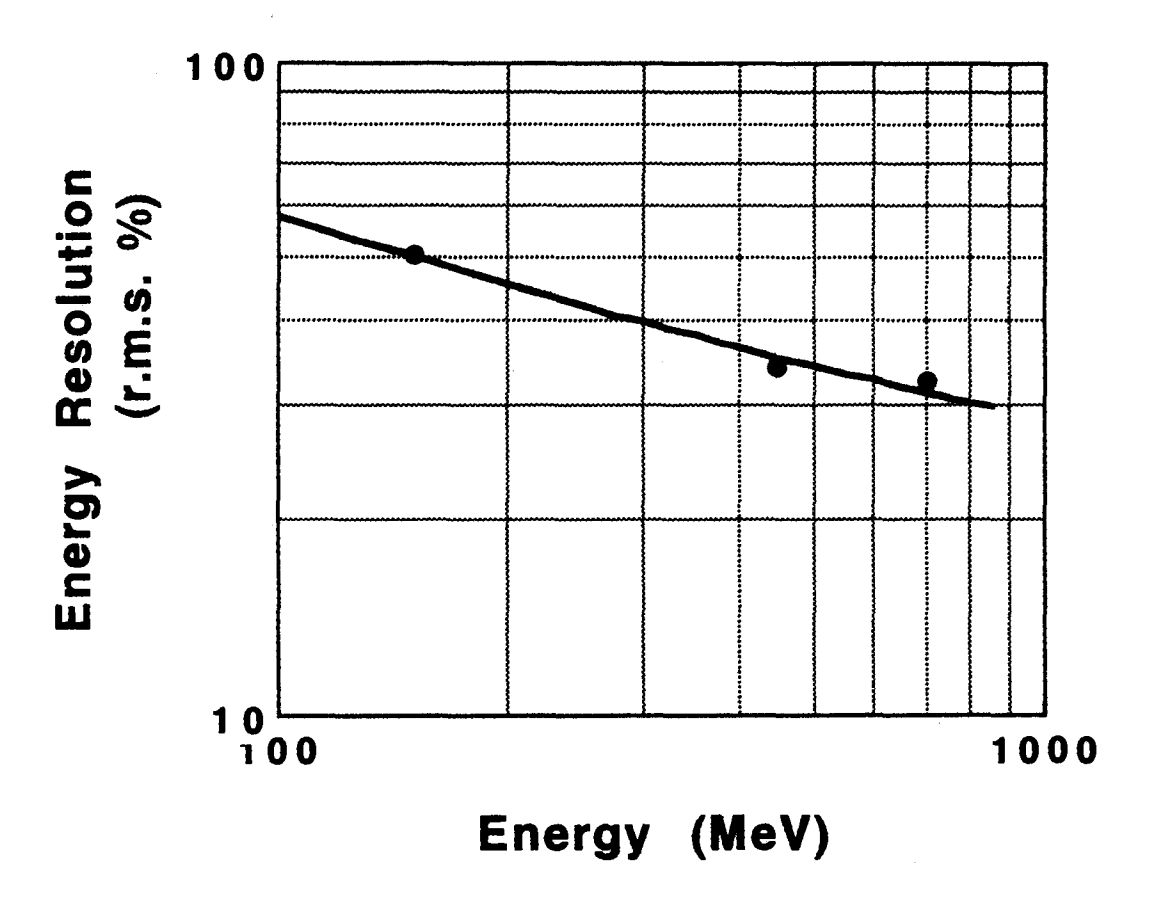


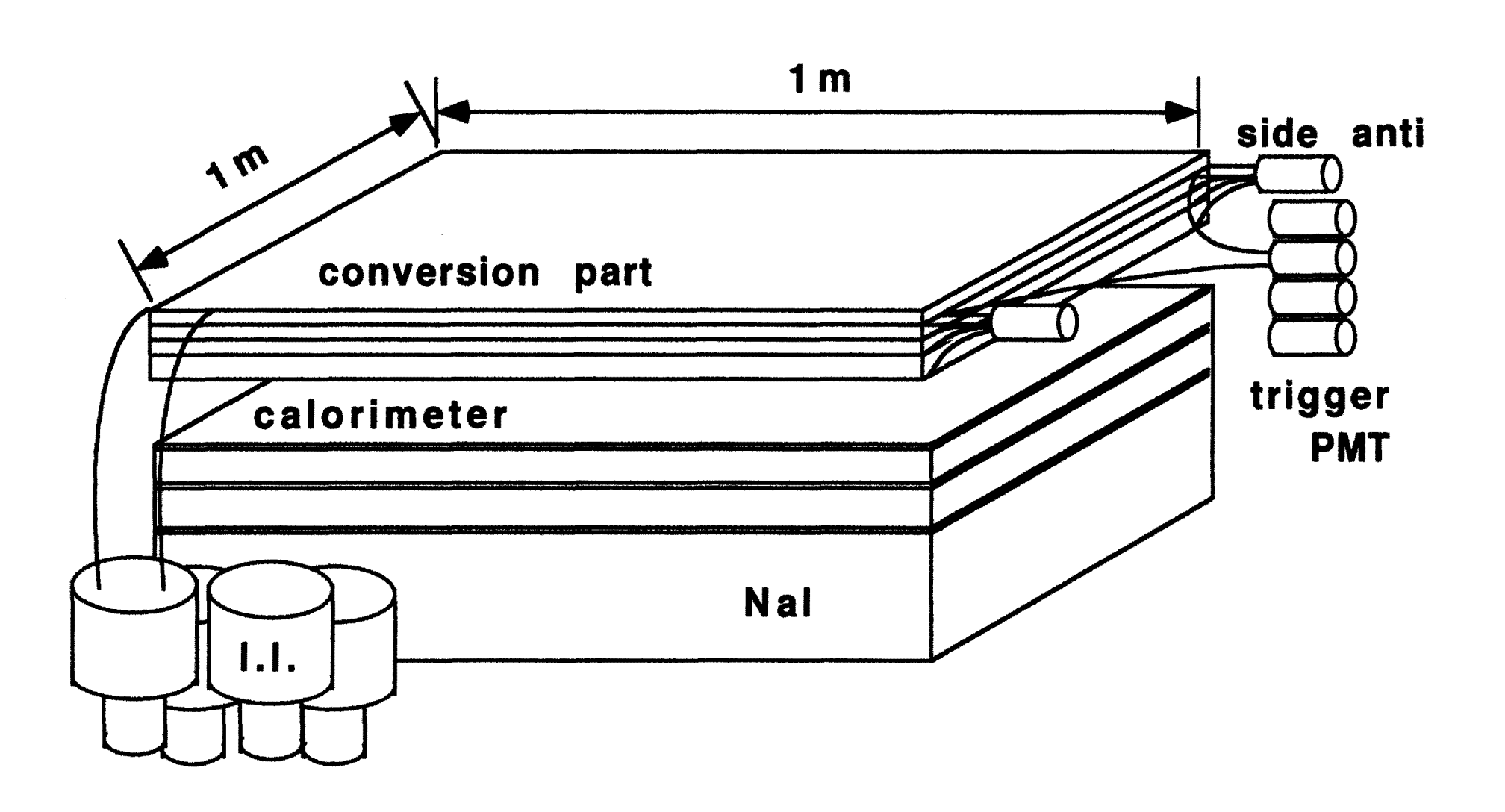


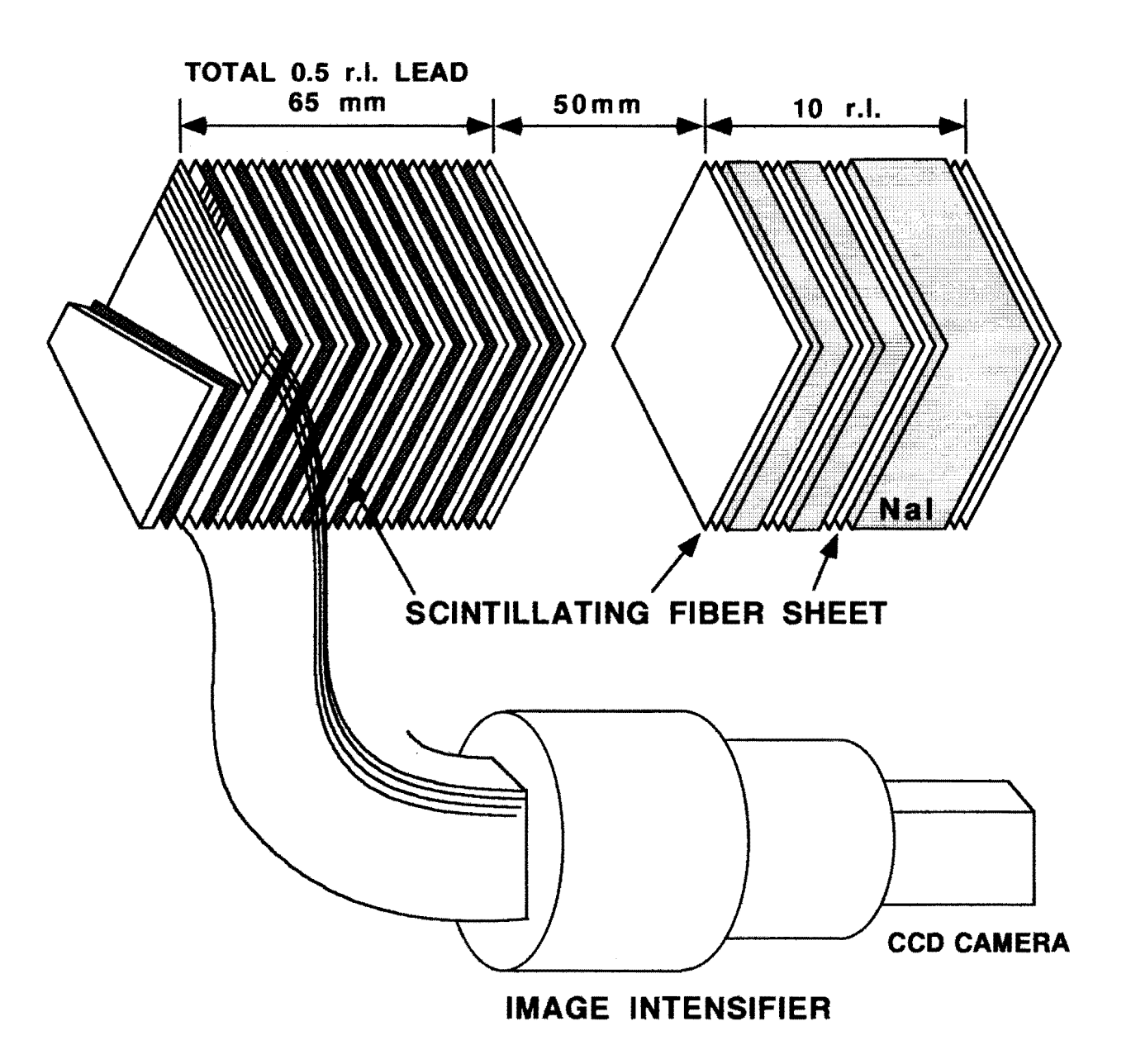
5-C (Now)

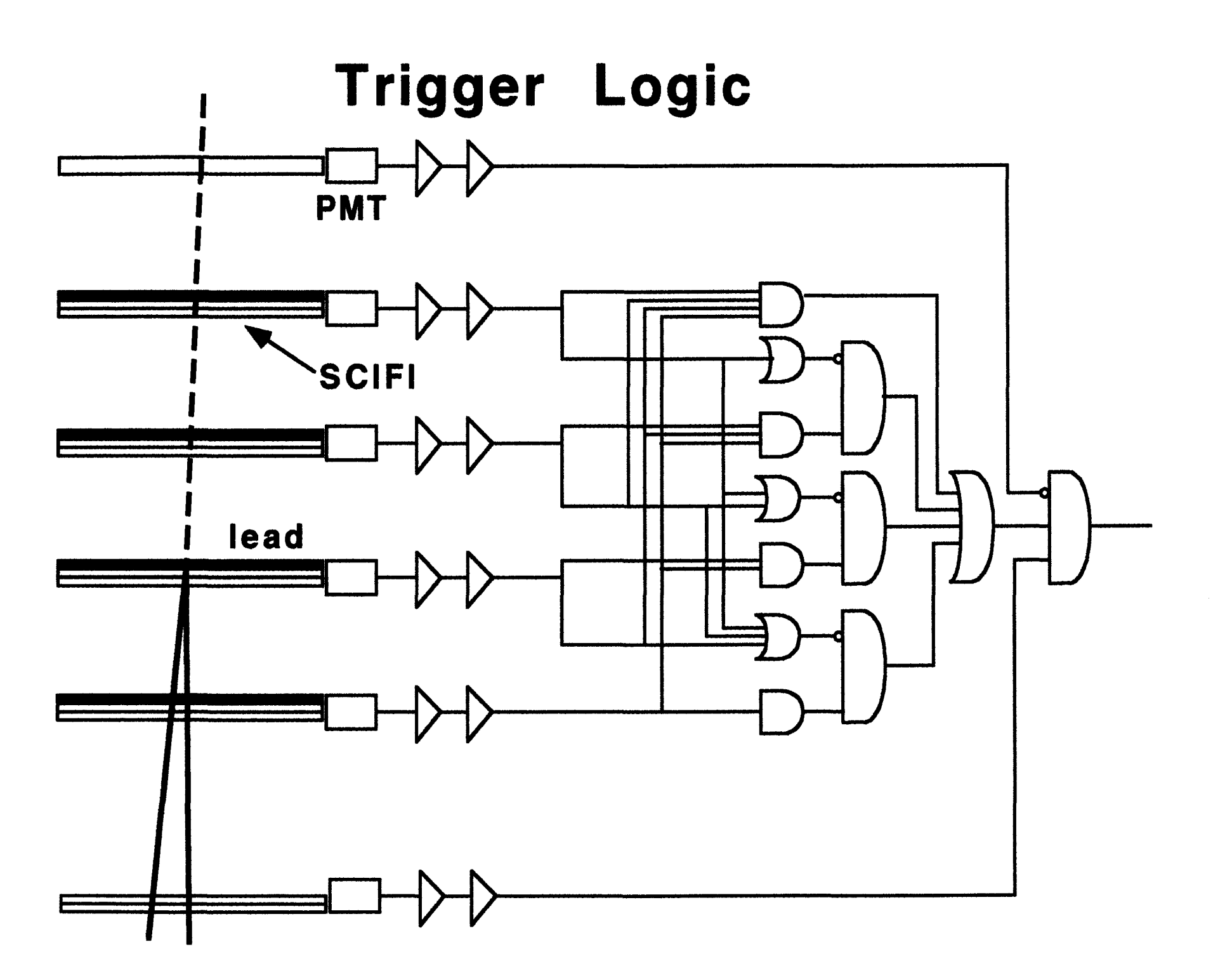












A

